ANTIOXIDANTS & REDOX SIGNALING
Volume 12, Number 3, 2010

DOI: 10.1089/ars.2009.2817

Intermediate Filament Carbonylation During Acute Acrolein Toxicity in A549 Lung Cells: Functional Consequences, Chaperone Redistribution, and Protection by Bisulfite

Philip C. Burcham, Albert Raso, and Colin A. Thompson

Abstract

Extensive protein carbonylation accompanies cellular exposure to acrolein, a ubiquitous smoke constituent implicated in life-threatening pulmonary edema in fire victims, a condition involving rapid erosion of the "watertight" properties of respiratory epithelium. Since the identities of lung epithelial proteins that sustain carbonylation by acrolein are unknown, we sought to identify significant targets in subcellular fractions from A549 cells after 30 min exposure to either subtoxic or acutely toxic acrolein concentrations (60 or 360 fmol acrolein/cell). The lower concentration mainly modified cytosolic proteins while the higher concentration also damaged nuclear, membrane, and cytoskeletal proteins. The multifunctional intermediate filament proteins vimentin, keratin-18, keratin-7 and keratin-8, were conspicuous targets. Consistent with their mechanical functions, a loss of cellular adhesive strength accompanied adduction of the two most abundant intermediate filaments in A549 cells, keratins-8 and -18. Acrolein also elicited redistribution of several chaperones (Hsp40, -70, -90, and -110) to intermediate filament fractions, suggesting chaperone-mediated autophagy contributes to the triage of acrolein-adducted proteins. The carbonyl scavenger bisulfite suppressed acrolein toxicity, intermediate filament adduction, vimentin cross-linking, Hsp90 redistribution, and loss of cellular adhesive strength, while also suppressing vimentin hyperphosphorylation. These novel observations identify intermediate filaments as key targets for the reactive smoke constituent acrolein. *Antioxid. Redox Signal.* 12, 337–347.

Introduction

Since high levels of acrolein are present in smoke formed on combustion of vegetation, timber, plastics, and building materials, this toxic 3-carbon electrophile is a key mediator of smoke inhalation injury (SII) in fire victims inhaling large doses of smoke (9). Pulmonary edema, a life-threatening consequence of acute damage to the epithelial lining of respiratory airways, is a major contributor to morbidity and mortality in SII. The clinical picture in SII is complex, but often involves a latency of 24–72 h, followed by bronchorrhea, bronchospasm, breathing abnormalities, and alveolar flooding (18). Although smoke is a complex cocktail of noxious substances, acrolein appears to play a clear pathogenetic role in SII-related pulmonary edema, a conclusion that is consistent with its strong reactivity towards lung epithelium (16, 17). Although several physiological mechanisms contribute to maintaining "dry" airspaces within the lung (33), how acrolein disrupts these processes to induce pulmonary edema is unclear.

The conjugated $\alpha\beta$-unsaturated bond of acrolein and related type-2 alkenes reacts readily with soft nucleophiles to form carbonyl-retaining Michael adducts (30). Reactions with glutathione are favored, but acrolein also attacks cysteine groups in proteins, ensuring that extensive protein carbonylation accompanies cell exposure to acrolein (4). Identifying targets for modification is worthwhile since such knowledge can provide mechanistic insight into cellular or metabolic pathways that are dysregulated by electrophiles. The cellular targets for other type-2 alkenes such as 4-hydroxynonenal (48)

Pharmacology and Anaesthesiology Unit, School of Medicine and Pharmacology, the University of Western Australia, Nedlands, Australia.

and the food contaminant acrylamide (2) are increasingly well defined, while recent proteomics studies have also identified various cytoskeleton-associated proteins as acrolein targets (29, 35). In a recent study, intravenous acrolein administration caused myocardial damage in mice, including adduction of sarcomere/cytoskeletal proteins and those involved in energy metabolism (31). At present, relationships between adduction of specific proteins and toxic cellular outcomes are unknown for acrolein, particularly in relation to protein targets within respiratory epithelium. The possibility that acrolein targets proteins involved in maintaining the "watertight" properties of the lung deserves serious attention.

The first aim of this work was to identify novel targets for acrolein within A549 lung epithelial cells, focusing on damage occurring under acutely toxic exposure conditions relevant to the high-dose exposure scenarios prevailing in SII (16, 17). Second, in an effort to evaluate the toxicological significance of damage to individual proteins, the carbonyl scavenger bisulfite was used to titrate modification of specific targets against deleterious cellular outcomes. A third aim was to explore cellular responses to the adduction of target proteins by studying the recruitment of molecular chaperones to cell extracts containing acrolein-modified proteins. The heat shock proteins hsp40, -70, -90, and 110 play broad roles in maintaining homeostasis during cell stress, including participation in the chaperone-mediated autophagic pathway for removing abnormal proteins (10, 37), but their roles in cellular responses to acrolein are unknown. Our collective results show that under exposure conditions eliciting acute toxicity, acrolein exhibits particular reactivity with intermediate filaments (IF), a family of proteins likely to perform important functions within lung epithelia. These components of the cytoskeleton differ from actin microfilaments and tubulin microtubules in terms of the large number of genes that encode them, their broad cellular distribution, relative insolubility, and diverse cellular functions (32, 38). Recent discoveries continue to extend known IF functions beyond their historically recognized role in the provision of mechanical strength to cells and tissues. The finding that several members of this protein family are targets for acrolein raises intriguing questions concerning the mechanistic significance of such damage to the diversity of biological processes in which IF participate.

Materials and Methods

Reagents

Sodium bisulfite, 17-(allylamine)-17-demethoxygeldanamycin (17-AAG), goat vimentin antiserum, monoclonal mouse antibodies against phospho-tyrosine, -serine and -threonine, as well as rabbit anti-DNP and anti-Hsp40 and Hsp110 sera were obtained from Sigma-Aldrich (St. Louis, MO). Rabbit Hsp90 and Hsp70 antibodies were purchased from Cell Signaling Technology (Danvers, MA). Peroxidase-coupled anti-rabbit Ig was supplied by Pierce (Rockford, IL). Acrolein was supplied by Alexis Biochemicals (Lausen, Switzerland). Dulbecco's phosphate-buffered saline (DPBS, glucose and pyruvate-containing) and dispase (*Bacillus polymyxa*, 1.75 units/mg) were purchased from GIBCO (Invitrogen Australia Pty Ltd, Mt Waverly, VIC). Sequencing grade trypsin from bovine pancreas was obtained from Roche (Kew, Victoria).

Cell culture

Human A549 adenocarcinoma lung cells (ATCC, Manassas, VA) were grown in F12K nutrient mixture supplemented with 10% FBS (vol/vol), gentamicin (100 μg/mL), and amphotericin B (2.5 μg/mL). The cells were harvested by trypsin-EDTA digestion and resuspended in F12K media supplemented with 0.5% FBS. Cell number was determined and cells were plated in 1.4 mL volumes on 6-well plates at a density of 0.6×10^6 cells per well. The plates were then maintained at 37°C in 5% CO_2 overnight before they were washed twice with Dulbecco's phosphate-buffered saline (DPBS) before commencing exposure to acrolein at final concentrations of 0, 25, 50, 75, 100, 150, or 200 μM. To avoid side-reactions with media constituents, cells were exposed to acrolein in DPBS solutions (45). Cell ATP levels were measured using a Promega CellTiter-Glo® Luminescent Cell Viability assay kit (Madison, WI) with luminescence readings taken using a PolarStar Optima microplate reader (BMG-Labtech, GmbH, Offenburg, Germany). In designated experiments, the hsp90 inhibitor 17-AAG was added to cell media to a final concentration of 1 μM.

To assess the stability of carbonylated IF, cells were exposed to acrolein (75 μM) for 30 min, after which unreacted aldehyde was removed by rinsing. Fresh solutions of F12K media containing 0.5% FBS were added before dishes were returned to the incubator.

Cell fractionation

To evaluate the subcellular distribution of early acrolein-induced protein damage, A549 monolayers were exposed to acrolein for 30 min before a *Q-Proteome Cell Fraction Kit* was used to prepare cytosolic, nuclear, membrane, and cytoskeletal fractions (Qiagen Pty. Ltd., Doncaster, Australia). Protein concentrations were determined using the BCA assay (Sigma-Aldrich). Intermediate filaments were isolated using a detergent extraction method that first involved rinsing A549 monolayers three times with Ca^{2+}- and Mg^{2+}-free PBS (50). A 10 mL volume of cell lysis solution was then added to each dish (Ca^{2+}- and Mg^{2+}-free PBS containing 0.6 M KCl, 1% Triton X-100, 10 mM $MgCl_2$, 1% β-mercaptoethanol, 1 mM PMSF, and 0.5 mg/mL p-tosyl-L-arginine methylester). DNase I was added to a final concentration of 0.5 mg/mL and the dishes were placed on ice for 5 min. The suspension was transferred to polypropylene tubes and centrifuged at 2,000 g for 10 min at 4°C, after which the supernatant was discarded. The IF-containing pellet was then washed via one round of centrifugation (3 min, 2,000 g) in Ca^{2+}- and Mg^{2+}-free PBS containing 0.1 mM PMSF and 1% β-mercaptoethanol before it was finally resuspended in 75 μL urea (6 M). Protein concentrations in 5 μL aliquots were then estimated using the BCA assay.

Peptide mass fingerprinting

To identify proteins of interest in cytoskeletal extracts, IF extract protein (100–200 μg/lane) was resolved on a large 12% polyacrylamide gel. Following electrophoresis and gel staining (*EZBlue™ Gel Staining Reagent*, Sigma-Aldrich, Australia), bands co-migrating with carbonylated targets in parallel immunoblots were excised from the gel. The gel fragments were destained and digested with trypsin before peptides were extracted using standard techniques (7). Peptides were ana-

lyzed using a MALDI-TOF/TOF mass spectrometer (4800 Proteomics Analyzer, Applied Biosystems, Foster City, CA) before the resulting mass spectra were processed using Mascot sequence matching software (Matrix Science, London, U.K.) (43).

Western blot analysis

Since the favored Michael addition chemistry forms carbonyl-retaining adducts, protein carbonyls are sensitive markers of acrolein-induced protein damage (4). For the evaluation of total protein carbonyls, cell proteins were extracted by adding 50 μL of 6 *M* urea to each dish. The contents were transferred to fresh tubes and, following brief sonication, 10 μL aliquots were assayed for protein content. Aliquots comprising 15 μg protein were treated with an equal volume of carbonyl derivatizing solution [0.5% 2,4-dinitrophenylhydrazine (wt/vol) in 10% trifluoroacetic acid (vol/vol)]. Subsequent steps including sample treatment, resolution on 7.5% PAGE gels, transfer to nitrocellulose, membrane blocking, antibody treatment, washing, and membrane development were as outlined previously (5). Chemiluminescence images were analyzed with Kodak Molecular Imaging software (Vs. 4.01). In experiments in which vimentin cross-linking, phosphoprotein status and heat shock protein recruitment were evaluated in IF extracts, proteins (20 μg/lane) were resolved on a 7.5% gel prior to electrophoretic transfer to nitrocellulose. Membrane blocking, immunorecognition, and washing were as recommended by the antibody suppliers, with primary rabbit antibodies used at 1/1,000 dilutions.

Dispase cell dissociation assay

The adhesive strength of A549 monolayers was evaluated using a modified version of published procedures (19, 21). Cells were grown to 1-day post-confluency on 60 mm dishes before they were washed with PBS and exposed to acrolein (0–200 μM) for 90 min in DPBS. The monolayers were rinsed 2X with PBS to remove unattached cells and then treated for 30 min at 37°C with 2 mL dispase solution (2.4 units/mL in DPBS). The enzyme solution was discarded and replaced with fresh PBS before cells were subjected to mild mechanical stress (20 oscillations on a shaking platform). The supernatant was then carefully transferred to 2 mL centrifuge tubes. Following centrifugation for 1 min at 2,600 *g*, pellets comprising dispase-released cells were resuspended in 1 mL PBS before they were subjected to an additional round of centrifugation and rinsing in PBS. The pellet was finally suspended in 100 μL sodium hydroxide (1.0 *M*) and digested in a hot water bath (70°C) before 10 μL aliquots of hydrolysate were analyzed for protein content using the BCA assay.

Statistics

Data were analyzed for significant differences by performing ANOVA followed by Tukey's post-hoc test using *SigmaStat for Windows* (Version 3.5) (Systat Software, San Jose, CA).

Results

Concentration-dependent protein damage and toxicity

Little is known concerning levels of free acrolein in the lung tissue of SII victims. In the case of burning tobacco, some indication of the dose of acrolein likely to be received is conveyed by the acrolein concentrations reported when smoke from a single cigarette was bubbled through 10 mL of buffered saline, namely 34–503 μM depending on the brand of cigarette tested (26). Our initial experiments thus sought to identify acrolein concentrations that elicited acute toxicity and protein modification (Fig. 1). A549 cells were exposed to 25–150 μM acrolein (*i.e.*, 60–360 fmol/cell) for 30 min before protein damage was detected via Western blotting (Fig. 1B). Separate dishes were used to assess cell viability via estimation of ATP levels after 4 h (Fig. 1B). Acrolein induced concentration-dependent loss of cell ATP while also modifying numerous cell proteins (Fig. 1A and B). Even concentrations of acrolein that did not diminish ATP levels during the 4 h duration of the experiment (25–75 μM) caused extensive protein carbonylation (Fig. 1B).

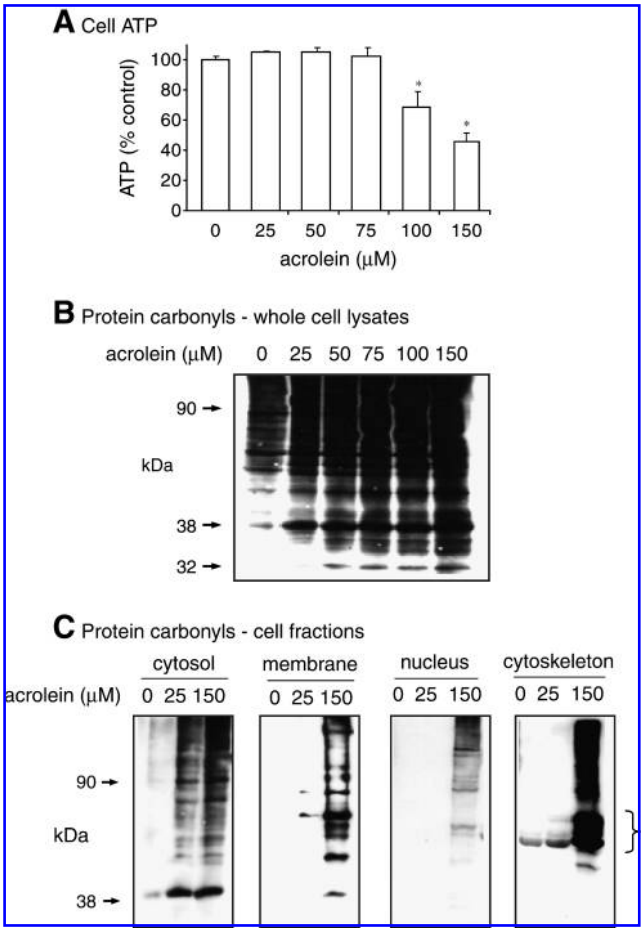

FIG. 1. Acrolein toxicity and protein carbonylation in A549 lung cells. (**A**) ATP levels after a 4 h exposure to 25–150 μM acrolein ($N = 4$, mean ± SE); A (*) indicates significantly different from controls ($p < 0.05$, Tukey's post hoc test). (**B**) Protein carbonyls in total cell lysates, and (**C**) subcellular fractions following a 30 min exposure to acrolein (15 μg protein/lane). Immunoblots shown are representative of four or more independent determinations.

Subcellular distribution of protein damage

To facilitate identification of individual acrolein targets, cells were fractionated into cytosolic, membrane, nuclear, and cytoskeletal extracts prior to protein carbonyl determination (Fig. 1C). Extracts were prepared after 30 min exposure to either an acrolein concentration that did not elicit overt toxicity (25 μM) or the 150 μM concentration that significantly decreased ATP levels (Fig. 1A). Consistent with the prevalence of protein cysteine groups in the reduced state within cytosol (*i.e.*, facile targets for soft electrophiles), cytosolic proteins were extensively modified by both the subtoxic and acutely toxic concentrations (Fig. 1C). In contrast, proteins in extracytosolic fractions (membrane, nuclear, and cytoskeletal) incurred minimal damage at the low acrolein concentration while showing substantial adduction at the high concentration (Fig. 1C). Cytoskeletal proteins were extensively damaged at the highest concentration (Fig. 1C). The extensive protein carbonylation elicited by low concentration acrolein in total cell extracts (Fig. 1B) thus seems to mainly reflect damage to abundant cytosolic proteins, with cell fractionation facilitating detection of damaged proteins in other cell compartments at higher exposure levels (Fig. 1C).

Characterization of IF damage

Peptide mass fingerprinting was first used to identify targets in cytoskeletal extracts prepared using the Q-Proteome Cell Fractionation kit (Qiagen, Doncaster, Victoria) (bands of interest in the ~45–55 kDa mass range are highlighted in Fig. 1C). Since the targets were tentatively identified as intermediate filament (IF) proteins, a detergent-based protocol was used to extract IF proteins after brief exposure of cells to a wider range of acrolein concentrations. Protein carbonyl analysis of the resulting IF extracts revealed four major targets (Fig. 2B), the identities of which were confirmed during a second round of peptide mass fingerprinting as vimentin and keratins-7, -8 and -18 (Table 1).

As in Fig. 1C, while four IF proteins were damaged by 150 μM acrolein (Fig. 2A), clear differences in susceptibility were evident at lower acrolein concentrations (Fig. 2C). To relate these findings to protein abundance, Fig. 2B depicts a Coomassie blue-stained gel obtained during SDS-PAGE of IF extracts from native A549 cells. Vimentin was only moderately abundant yet highly vulnerable to modification, showing saturation of adduction at the lowest acrolein concentration (25 μM, Fig. 2C). The least abundant of the four IF targets (Fig. 2B), keratin-7, was highly susceptible, exhibiting saturation of adduction at 50 μM and higher acrolein concentrations (Fig. 2A and C). In contrast, keratins-8 and -18 were highly abundant (Fig. 2B) yet only incurred substantial damage at the most acutely toxic concentrations (Fig. 2A and C).

Differential protection of individual IF proteins by bisulfite

Since bisulfite strongly inhibits acrolein-mediated protein adduction and toxicity (5), this scavenger was used to explore relationships between cytoprotection and protection of specific IF targets (Fig. 3). Bisulfite strongly suppressed cellular ATP depletion elicited by a 4 h exposure to 150 μM acrolein, with 50 μM and higher bisulfite concentrations completely preventing ATP loss (Fig. 3A). Suppression of IF carbonylation accompanied the cytoprotection, with the greatest protection at mid-range concentrations afforded towards the most abundant yet least susceptible IF targets, keratins-8 and -18 (Fig. 3B and C). The most vulnerable IF targets, vimentin and keratin-7, were only fully protected at the highest bisulfite concentration. Cytoprotection thus appeared to correlate with protection of the most abundant IF targets rather than the most vulnerable IF species.

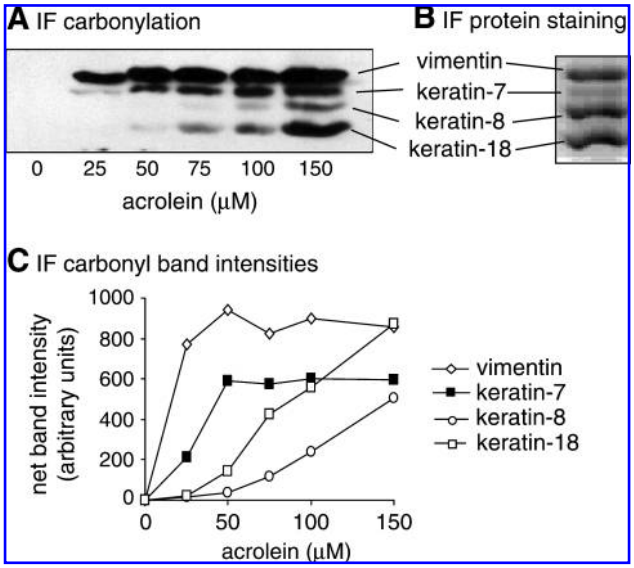

FIG. 2. Concentration-dependent carbonylation of vimentin and keratins by acrolein in A549 cells. (**A**) Carbonyls in IF extract proteins (15 μg/lane) exposed to 25–150 μM acrolein for 30 min; (**B**) Coomassie blue stained IF extract from native A549 cells, and (**C**) band intensity from carbonylated IF. Immunoblots shown are representative of four or more independent determinations.

Vimentin cross-linking

In recent work, formation of high-mass protein aggregates coincided with the loss of carbonylated proteins in cells sub-

Table 1. Proteins Identified during Proteomic Analysis of Bands Co-migrating with Carbonylated Species in IF Extracts from Acrolein-Treated A549 Cells

*Protein identity**	*Protein score*†	*Confidence interval (%)*	*Mass (kDa)*‡	*IEP (pH)*	*Peptide count*§
Keratin-18	134	100	47.3	5.27	17
Keratin-8	149	100	53.7	5.52	20
Keratin-7	73	99.364	51.4	5.42	12
Vimentin	76	99.696	49.6	5.19	12

*Identity of protein with greatest number of peptide matches within band of interest.

†Mowse score determined from peptide mass fingerprinting. Protein scores greater than 72 are significant ($p < 0.05$).

‡Post-translational modifications (*e.g.*, glycosylation) may contribute to differences in the order of IF protein migration during SDS/PAGE compared to expectations based on mass estimates.

§Number of peptides matched.

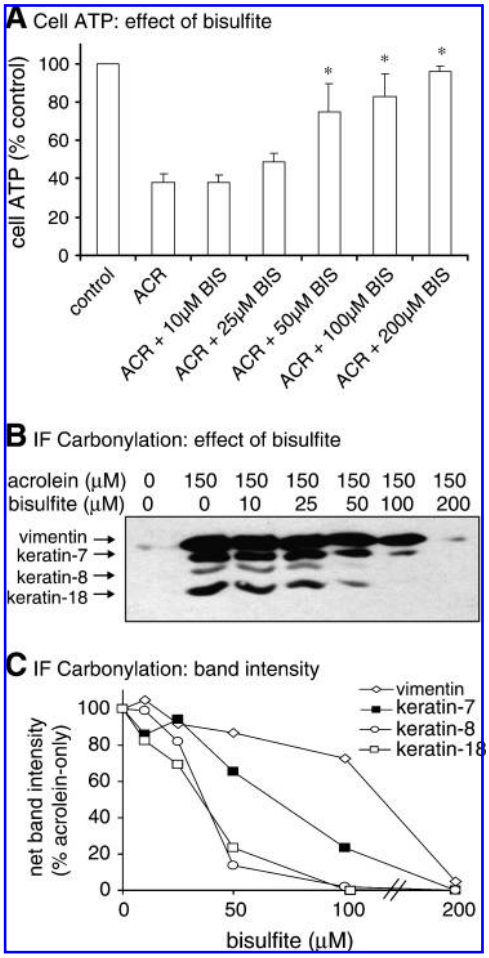

FIG. 3. Bisulfite protects against acrolein-induced toxicity and IF carbonylation in A549 cells. (**A**) ATP levels after a 4 h exposure to 150 μM acrolein in the presence of 10–200 μM bisulfite. A (*) indicates a significant difference from controls ($p < 0.05$, Tukey's post hoc test); (**B**) carbonyl levels in IF proteins after a 30 min exposure (15 μg protein/lane), and (**C**) band intensity of carbonylated IF proteins. Immunoblots shown are representative of three or more independent determinations.

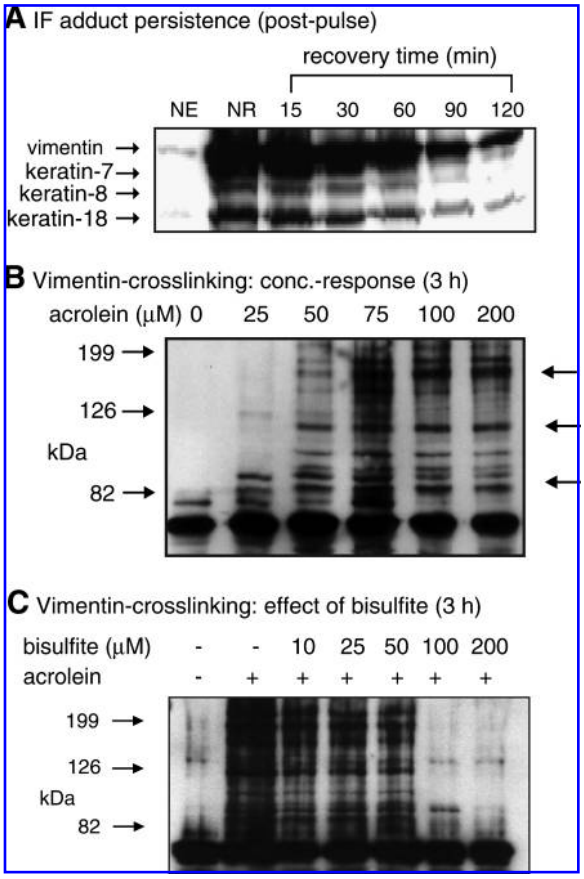

FIG. 4. Acrolein-induced formation of vimentin-containing high-mass species and protection by bisulfite. (**A**) Time-course of loss of carbonylated IF in cells recovering from a prior 30 min exposure to 75 μM acrolein (15 μg protein/lane). NE, no exposure; NR, no recovery. (**B**) Western blot obtained with anti-vimentin antibody showing formation of high-mass species (*arrows*) within IF extracts from A549 cells after a 3 h exposure to acrolein. (**C**) Co-incubation of acrolein with cytoprotective bisulfite concentrations suppress vimentin-crosslink formation. The immunoblots in (A) and (B) were obtained with anti-vimentin antibody and depict 20 μg protein/lane (representative of three or more independent determinations).

jected to brief acrolein exposure followed by recovery in aldehyde-free media (5). To determine whether carbonyl IF adducts undergo similar decay, A549 cells were exposed to a 30 min pulse of acrolein before they were washed and allowed to recover for up to 2 h in acrolein-free media (Fig. 4A). As in recent studies of the reversibility of Michael adducts at cysteine (28), the intensity of carbonylated IF targets declined during the recovery period (Fig. 4A).

The possibility that the decline in IF carbonyl adducts might involve cross-linking reactions was confirmed by the detection of vimentin-containing aggregates after 3 h exposure to acrolein (Fig. 4B). Intriguingly, acrolein elicited concentration-dependent increases in the mass of aggregated products, suggesting acrolein-adducted vimentin cross-linked with distinct proteins under different exposure conditions (arrows highlight several vimentin-containing bands in Fig. 4B). Consistent with their ability to suppress vimentin adduction (Fig. 3B), high bisulfite concentrations strongly inhibited vimentin cross-linking (Fig. 4C).

Consequences of IF damage

Phosphorylation regulates many IF functions, including the organization and solubility of filament networks, interactions with accessory proteins, and roles in cellular adhesion, cell death, and vectorial transport (32, 39). To determine whether the phosphorylation status of IF targets alter during toxicity, Western blotting was used to evaluate IF phosphotyrosine levels in cells after a 30 min exposure to acrolein (Fig. 5A). Despite its susceptibility to adduction (Fig. 2A), phosphotyrosine levels in vimentin only increased at the acutely toxic 150 μM concentration (Fig. 5A). Phosphotyrosine levels in the other three IF targets were unaltered by 100 μM and lower concentrations of acrolein (Fig. 5A). A 30 min exposure

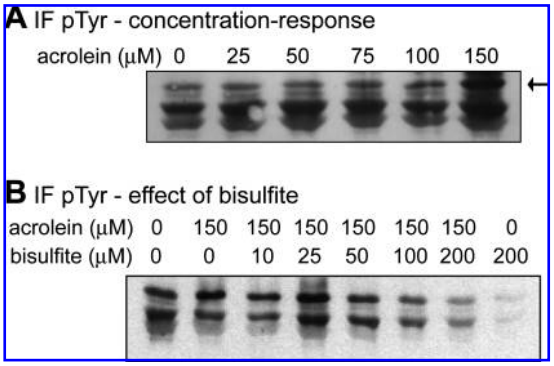

FIG. 5. Western blot showing vimentin tyrosine hyperphosphorylation during acrolein exposure and suppression by bisulfite. (**A**) IF extracts prepared following a 30 min exposure of A549 cells to 25–150 μM acrolein were evaluated for phosphorylation status using an anti-phosphotyrosine antibody (*arrow* highlights the hyperphosphorylated vimentin band). (**B**) Bisulfite suppresses basal and acrolein-induced vimentin phosphorylation; 20 μg protein/lane in (A) and (B). Immunoblots shown are representative of three or more independent determinations.

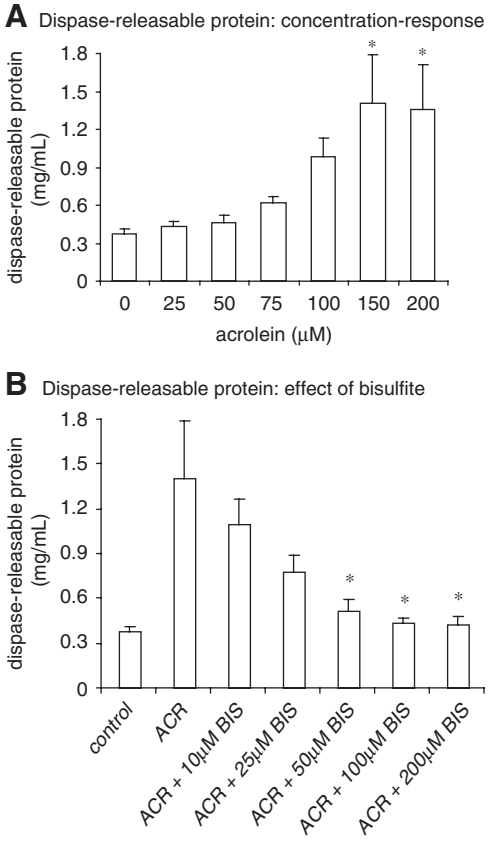

FIG. 6. Acrolein-induced loss of cellular adhesive strength and prevention by bisulfite. (**A**) Dispase-releasable protein from confluent A549 monolayers after 90 min exposure to acrolein (25–200 μM) prior to dispase treatment (30 min) and subjection to mild mechanical stress. (**B**) Protection by bisulfite against the loss of cellular adhesive strength elicited by a 90 min exposure to 150 μM acrolein. The values shown are mean $\pm$ SE from three to four independent experiments.

to 25–150 μM acrolein also failed to alter phosphoserine or phosphothreonine levels in the four IF targets (data not shown). The highest bisulfite concentrations strongly suppressed vimentin hyperphosphorylation during a 30 min exposure to 150 μM acrolein (Fig. 5B).

A 90 min exposure to acrolein diminished the adhesive strength of A549 monolayers, as revealed by the increase in dispase-releasable proteins in monolayers subjected to mild mechanical stress (Fig. 6A). Significant reductions were produced by high concentrations that carbonylated the most prevalent IF proteins, keratin-8 and −18 (*i.e.*, 100 μM and higher, Fig. 3B). Consistent with their ability to protect keratins-8 and -18, 50 μM and higher bisulfite concentrations blocked the loss of cellular adhesive strength induced by 150 μM acrolein (Fig. 6B).

Molecular chaperone redistribution

To establish whether acrolein elicits chaperone redistribution to damaged IF, Western blotting was used to detect Hsp110, Hsp90, Hsp70, and Hsp40 in IF fractions from acrolein-treated cells (Fig. 7). As with previous reports, Hsp70 was associated with IF in control cells (27). A 3 h exposure to acrolein caused concentration-dependent increases in all chaperones within IF fractions (Fig. 7A–D). A clear threshold applied to the response, since while 25 μM acrolein strongly modified vimentin (Fig. 2A), this concentration did not increase chaperone levels within IF extracts (Fig. 7A–D). In contrast, 50, 75, and 100 μM acrolein modestly increased IF-associated levels of all four chaperones, with Hsp40 the most strongly responsive marker at these concentrations (Fig. 7A–D). Consistent with the extensive IF damage it caused, 150 μM acrolein strongly increased IF-associated levels of the two large chaperones, Hsp90 and -110 (Fig. 7C and D).

In the case of Hsp90, high acrolein concentrations also promoted the formation of high-mass Hsp90-containing species that displayed a mass of ~180–190 kD during SDS/PAGE (Fig. 7A and B). It is likely this product formed via intermolecular cross-linking during the processing of damaged proteins by Hsp90-containing complexes (see below).

Consistent with its ability to block IF adduction, bisulfite strongly inhibited acrolein-induced chaperone recruitment to IF extracts (Fig. 7A–D). In general, only the two highest concentrations of bisulfite suppressed the increases in IF-associated chaperones (Fig. 7C). Since these concentrations protected the two most abundant IF targets (Fig. 3B and C), together with the finding that no chaperone redistribution was elicited by the 25 μM acrolein concentration which damaged vimentin, chaperone redistribution to IF may primarily occur upon damage to abundant IF proteins. Bisulfite also attenuated formation of high-mass Hsp90-containing species in acrolein-treated cells (Fig. 7C).

Effect of Hsp90 inhibitor

To clarify mechanisms underlying chaperone redistribution to acrolein-adducted IF, and determine whether this phenomenon influences toxic responses to acrolein, the effects of the hsp90 antagonist 17-AAG on acrolein-induced ATP depletion (Fig. 8A) and IF-associated Hsp90 (Fig. 8B) were examined. The hsp90 inhibitor enhanced acrolein-induced

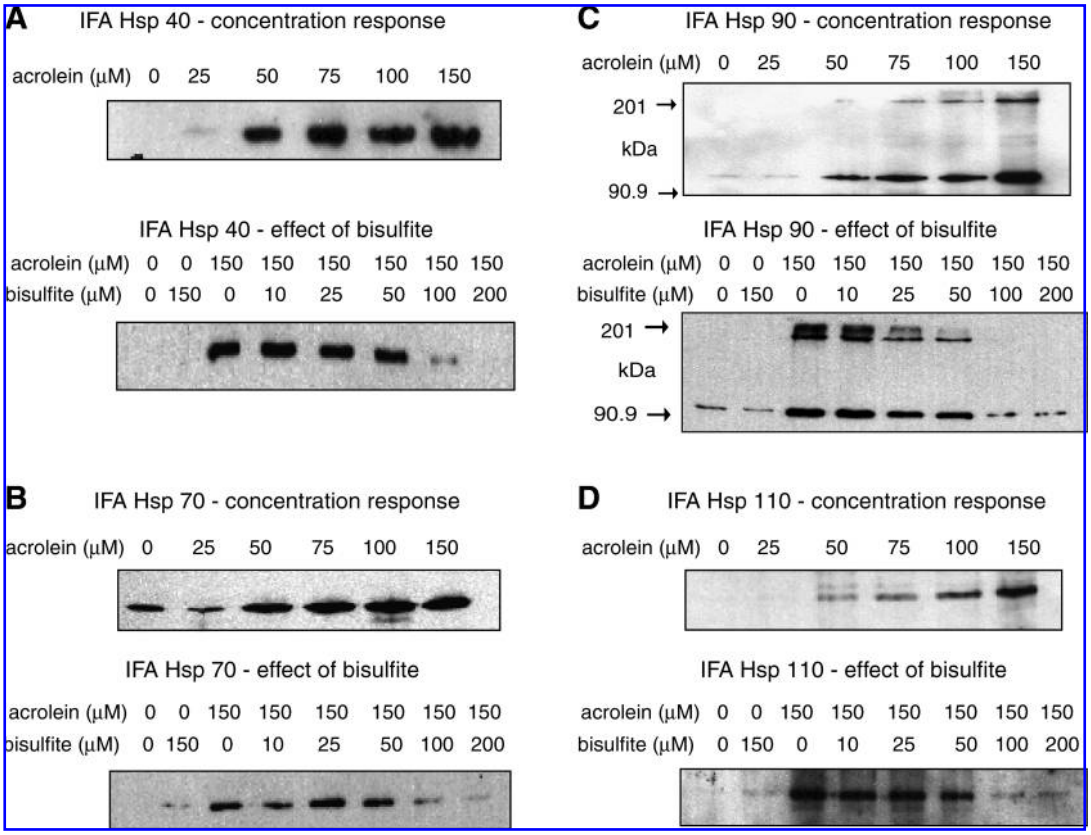

FIG. 7. Western blotting with anti-Hsp sera reveals acrolein-induced redistribution of molecular chaperones to IF extracts in A549 cells. The panels depict concentration-response curves (*upper blot*) and effects of bisulfite (*lower blot*) on the redistribution of Hsp40 (**A**), Hsp70 (**B**), Hsp90 (**C**), and Hsp110 (**D**) to IF extracts prepared from A549 cells after a 3 h exposure to acrolein (20 μg IF protein/lane in each panel). Immunoblots shown are representative of two or three independent determinations.

ATP depletion across a range of acrolein concentrations (Fig. 8A). While 17-AAG did not prevent acrolein-induced redistribution of monomeric Hsp90 to IF, the inhibitor did block formation of high-mass Hsp90-containing aggregate (Fig. 8B).

To determine whether Hsp90 redistribution was a generalized cellular response to acrolein exposure, Hsp90 levels were measured in various fractions prepared after a 3 h treatment with 150 μM acrolein (Fig. 8C). Intriguingly, Hsp90 was present in cytosolic extracts from both control and acrolein-treated cells, although acrolein treatment strongly increased levels of high-mass Hsp90-containing species in this extract (Fig. 8C). Hsp90 was not detected in either nuclear or membrane extracts from control or acrolein-treated cells (Fig. 8C). In contrast, Hsp90 levels strongly increased in cytoskeletal extracts during acrolein exposure (Fig. 8C), suggesting chaperone redistribution directly follows damage to these cell constituents.

Discussion

The over 65 members of the IF class belong to five subfamilies, of which all possess an α-helical rod domain flanked by N-terminal head and C-terminal tail domains (40). The highly conserved rod domains promote formation of coiled-coil dimer structures while the head and tail domains contain motifs that interact with adaptor proteins, ensuring IF act as scaffolds for many cell-signaling molecules (24). The terminal domains include phosphorylation motifs that are targets for various kinases including stress-activated kinases, suggesting one function of IF proteins includes an ability to act as "phosphate sponges" during cellular stress (20, 39). Our study breaks new ground by implicating members of three IF subfamilies as targets for acrolein, namely keratins-18 ("acidic" or Type-1 IF family), -7 and -8 ("basic" or Type-2) and vimentin (Type-3). Assuming similar damage occurs *in vivo*, the finding that lung epithelial cell IF are very susceptible to acrolein adduction could have mechanistic ramifications for SII pathogenesis.

Vimentin was especially vulnerable to acrolein, showing saturation of adduction at the lowest concentration studied (25 μM, Fig. 2B). Vimentin is expressed in endothelial and mesenchymal tissues where it participates in cell–cell attachment, cell differentiation, stress responses, cell signaling, and cell motility (22). Emerging as a common target for reactive electrophiles, vimentin is attacked by species as diverse as the thiol oxidant diamide (13); sugar-derived glycoxidation products (25); cyclopentanone prostaglandins (14); the antitumor alkaloid withaferin A (3), and quinone methide tumour promoters (33). Vimentin is thus vulnerable both to comparatively "hard" electrophiles which preferentially target lysine (*e.g.*, glyoxal) (25) and also "softer" electrophiles that attack cysteine (*e.g.*, PGA1) (14). Acrolein modifies both lysine and cysteine residues, although reactivity with the latter is favored on kinetic grounds (5). The divergent roles vimentin plays in

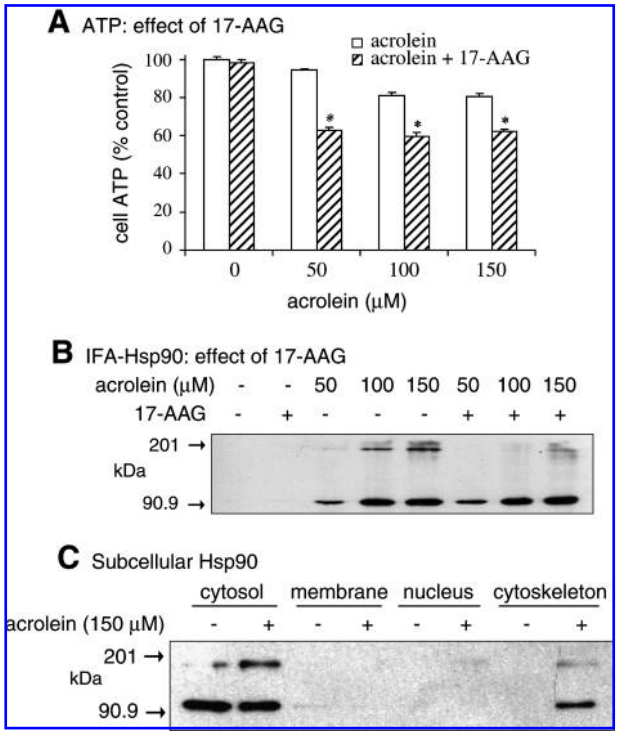

FIG. 8. Effects of 17-AAG on acrolein-induced ATP depletion and Hsp90 redistribution and crosslinking. (**A**) ATP levels at 4 h, and (**B**) IF-associated Hsp90 at 3 h following exposure to 50, 100, or 150 μM acrolein with and without co-exposure to 1 μM 17-AAG [$N = 4$, mean ± SE]. (**C**) Hsp90 levels in various subcellular fractions following a 3 h exposure to acrolein. In (A), a (*) indicates significantly different from controls ($p < 0.05$, Tukey's post hoc test). Immunoblots shown are representative of two or three independent determinations.

different tissues complicates the question of whether such damage compromises vimentin functionality. Recent work using human fibroblasts found the sugar-derived electrophile glyoxal targets lysine groups in linker regions of coiled-coil domains of the rod region of vimentin (25). Redistribution of vimentin to perinuclear globular aggresomal structures occurred on exposing fibroblasts to glyoxal, suggesting damage within rod domains disrupted IF dimerization and assembly (25). In our study, use of fluorescent immunohistochemistry did not reveal vimentin reorganization during 4 h exposures of A549 cells to acrolein (data not shown). This may suggest acrolein modification occurs in head or tail domains that are less important in oligomerization than the rod domain residues attacked by glyoxal.

Semiflexible intracellular IF networks help provide tensile strength to tissues subjected to mechanical deformations (49). These properties not only reflect IF interactions with neighboring IF proteins within polymeric networks, but also their ability to form linkages with cytoplasmic domains of integrin and other membrane-spanning anchor complexes. IF thus interact with a range of cell adhesion structures including desmosomes, hemidesmosomes, and matrix adhesions (22). To determine whether acrolein-induced IF damage disrupts such functions, cellular adhesive strength was evaluated in A549 cell monolayers using the dispase dissociation assay, a common method for assessing the phenotypic impact of keratin mutations (19, 21). Although adduction of the most vulnerable IF proteins, vimentin and keratin-7, appeared saturated at the 50 μM concentration, a loss of cellular adhesive strength only occurred at acrolein concentrations that damaged the more abundant IF proteins, keratins-8 and -18 (Figs. 2B and 6A). This suggests the mechanical roles of vimentin are subtle in the A549 cells, a conclusion concurring with findings made during studies of the phenotype of vimentin($^{-/-}$) cells (11).

The fact that keratins-8/-18 sustained adduction at acrolein concentrations that decreased cellular adhesive strength is consistent with the mechanical roles of keratins in many cell types (32, 38, 42). Keratins-8 and -18 are often co-expressed as IF heterodimers within epithelial cells which typically express at least one Type-1 (*e.g.*, keratin-18) and one Type-2 IF (*e.g.*, keratin-8). Keratins-8 and -18 are especially important in liver, with mutations in these genes accompanying various enterohepatic disorders (38). If keratin-8 and -18 adduction by acrolein extends to intact lung—a tissue subjected to mechanical forces during the normal breathing cycle—any disruption of keratin-containing IF networks and associated cell-cell attachment might conceivably erode the "watertight" properties of respiratory epithelium. The availability of lung epithelial cell lines that form excellent tight junctions may allow better testing of this idea (15).

The recent finding that inhalational acrolein exposure caused adduction of mouse vascular proteins (8) is intriguing given that keratin-7, a preferred target for acrolein identified in our study, is mainly expressed in endothelial tissues including the lining of blood vessels (36). To the best of our knowledge, keratin-7 has not previously been identified as a target for electrophiles.

The levels of carbonylated adducts declined in IF targets following a brief exposure to acrolein (Fig. 4A). Several mechanisms may contribute to this loss, including chemical reversal of the Michael addition reaction, proteolytic degradation of damaged proteins, or consumption of the carbonyl group during reactions with neighbouring nucleophiles (5). Concurring with the latter, adducted vimentin participated in diverse cross-linking reactions, with an unexpected concentration-dependence in the mass of the aggregates formed (Fig. 4B). At 25 μM acrolein, two bands formed that increased vimentin's mass by just 10–20 kDa, yet at 50 μM, a band with an additional mass of ~60–70 kDa appeared (Fig. 4B). At the most toxic acrolein concentrations (100 and 150 μM), a series of poorly resolved high-mass species exhibiting an additional mass of ~120–130 kDa formed (Fig. 4B). These observations suggest cells may tolerate formation of low mass vimentin-containing aggregates, while high-mass species are deleterious to cell viability.

The finding that acrolein carbonylated many cytosolic proteins (Fig. 1B) raised the possibility that a common pathway for clearing abnormal proteins from cytoplasm, chaperone-mediated autophagy (CMA), would be activated during acrolein toxicity. This pathway removes individual proteins via lysosomal proteolysis and is triggered by stresses that promote protein unfolding and exposure of hydrophobic KFERQ-like pentapeptide sequences within substrate proteins (10). The resulting recruitment of chaperones and co-chaperones promotes formation of complexes comprising Hsp70, Hsp90, Hsp40, Hop, Bag-1, and other proteins,

enabling further substrate unfolding and translocation to lysosomes. While the role of CMA in cellular responses to electrophiles is poorly characterized, prooxidant chemicals can activate CMA in some cell types (23). Our finding of increased chaperones in IF extracts from acrolein-treated cells suggests acrolein triggers chaperone mobilization in an effort to "buffer" damaged and destabilized IF proteins. However the hsp90 inhibitor 17-AAG failed to block hsp90 redistribution to IF extracts, indicating this response was independent of the conformational cycle of Hsp90. ATP-competitive inhibitors disrupt ATP-driven hsp90 dimerization, preventing "molecular clamp" interactions with client proteins (41).

The fact that 17-AAG blocked formation of high-mass hsp90-containing aggregates in cells exposed to toxic acrolein concentrations suggests controlled cross-linking events underlie formation of this high-mass species (Figs. 7 and 8). Upon ATP binding to hsp90 homodimers during the conformational cycle of hsp90, the two N-terminal ATP-binding domains are brought into close proximity (44). Our observations resemble recent findings from reconstituted *in vitro* systems comprising yeast Hsp90 and human Hsp90β where in the presence of ATP or a nonhydrolyzable ATP analogue, the cross-linking reagent dimethyl suberimidate generated high-mass Hsp90-containing species (46). Disruption of N-terminal dimerization using geldanamycin, an Hsp90 inhibitor with affinity for the ATP-binding site, reduced the yield of high mass species (46). Our analogous findings in intact lung cells provide powerful evidence for the transient dimerization of Hsp90 molecules during protein triage within the cellular environment.

Recent years has seen increasing interest in the use of nucleophilic reagents as carbonyl-sequestering drugs (1, 6). In earlier work, bisulfite was identified as an efficient acrolein-scavenger and inhibitor of protein carbonylation during acrolein toxicity (5, 47). Bisulfite rapidly traps acrolein to form propanal-3-sulfonate in the first instance (12). The present work extends these findings by showing that bisulfite strongly protected against acrolein-induced carbonylation of specific IF targets (Fig. 2B and C), blocked vimentin cross-linking (Fig. 3C), suppressed vimentin hyperphosphorylation (Fig. 5B), prevented the loss of adhesive cell strength (Fig. 6B), and prevented redistribution of chaperones to IF (Fig. 7). Collectively, these data indicate that bisulfite complements endogenous cellular electrophile-scavenging systems such as the glutathione-S-transferase pathway to trap acrolein within the intracellular environment at a rate that competes with the kinetics of the reaction of acrolein with protein targets.

In conclusion, acrolein displays strong reactivity with IF, with vimentin and keratin-7 favored targets at low concentrations, while keratins-8 and -18 sustained damage at higher acrolein concentrations. Since these cytoskeletal proteins play diverse cellular roles, they deserve further attention as key targets for electrophilic carbonyls in a wide range of disease states. In particular, future work should address the possibility that adduction compromises the ability of IF networks to provide tensile strength to respiratory epithelium in the smoke-exposed lung. Such pathogenetic mechanisms would represent a novel functional outcome of fundamental chemical events occurring in the early stages of acrolein exposure.

Acknowledgments

The authors are grateful for financial support for this work from the National Health and Medical Research Council of Australia (Project Grant ID 403967). The assistance of staff at Proteomics International Pty Ltd (Perth, WA, Australia) is gratefully acknowledged.

Author Disclosure Statement

No competing financial interests exist for any of the authors.

References

1. Aldini G, Dalle-Donne I, Colombo R, Maffei Facino R, Milzani A, and Carini M. Lipoxidation-derived reactive carbonyl species as potential drug targets in preventing protein carbonylation and related cellular dysfunction. *Chem Med Chem* 1: 1045–1058, 2006.
2. Barber DS, Stevens S, and LoPachin RM. Proteomic analysis of rat striatal synaptosomes during acrylamide intoxication at a low dose rate. *Toxicol Sci* 100: 156–167, 2007.
3. Bargagna-Mohan P, Hamza A, Kim YE, Khuan Abby Ho Y, Mor-Vaknin N, Wendschlag N, Liu J, Evans RM, Markovitz DM, Zhan CG, Kim KB, and Mohan R. The tumor inhibitor and antiangiogenic agent withaferin A targets the intermediate filament protein vimentin. *Chem Biol* 14: 623–634, 2007.
4. Burcham PC and Fontaine F. Extensive protein carbonylation precedes acrolein-mediated cell death in mouse hepatocytes. *J Biochem Mol Toxicol* 15: 309–316, 2001.
5. Burcham PC, Raso A, Thompson C, and Tan D. Intermolecular protein cross-linking during acrolein toxicity: Efficacy of carbonyl scavengers as inhibitors of heat shock protein-90 cross-linking in A549 cells. *Chem Res Toxicol* 20: 1629–1637, 2007.
6. Burcham PC. Potentialities and pitfalls accompanying chemico-pharmacological strategies against endogenous electrophiles and carbonyl stress. *Chem Res Toxicol* 21: 779–786, 2008.
7. Casey TM, Arthur PG, and Bogoyevitch MA. Proteomic analysis reveals different protein changes during Endothelin-1- or Leukemic Inhibitory Factor-induced hypertrophy of cardiomyocytes *in vitro*. *Mol Cell Proteomics* 4: 651–661, 2005.
8. Conklin DJ, Haberzettl P, Prough RA, and Bhatnagar A. Glutathione S-transferase P protects against endothelial dysfunction induced by exposure to tobacco smoke. *Am J Physiol Heart Circ Physiol* 296: H1586–H1597, 2009.
9. Demling RH. Smoke inhalation injury: An update. *J Plastic Surg* 8: 254–282, 2008.
10. Dice JF. Chaperone-mediated autophagy. *Autophagy* 3: 295–299, 2007.
11. Evans RM. Vimentin: The conundrum of the intermediate filament gene family. *BioEssays* 20: 79–86, 199.
12. Finch HD. Bisulfite adducts of acrolein. *J Org Chem* 27: 649–651, 1962.
13. Fratelli M, Demol H, Puype M, Casagrande S, Eberini I, Salmona M, Bonetto V, Mengozzi M, Duffieux F, Miclet E, Bachi A, Vandekerckhove J, Gianazza E, and Ghezzi P. Identification by redox proteomics of glutathionylated proteins in oxidatively stressed human T lymphocytes. *Proc Natl Acad Sci USA* 99: 3505–3510, 2002.
14. Gharbi S, Garzón B, Gayarre J, Timms J, and Pérez-Sala D. Study of protein targets for covalent modification by the antitumoral and anti-inflammatory prostaglandin PGA_1: Focus on vimentin. *J Mass Spectrom* 42: 1474–1484, 2007.

15. Grainger CI, Greenwell LL, Lockley DJ, Martin GP, and Forbes B. Culture of Calu-3 cells at the air liquid interface provides a representative model of the airway epithelial barrier. *Pharm Res* 23: 1482–1490, 2006.
16. Hales CA, Barkin PW, Jung W, Trautman E, Lamborghini D, Herrig N, and Burke J. Synthetic smoke with acrolein but not HCl produces pulmonary edema. *J Appl Physiol* 64: 1121–1133, 1988.
17. Hales CA, Musto SW, Janssens S, Jung W, Quinn DA, Witten M. Smoke aldehyde component influences pulmonary edema. *J Appl Physiol* 72: 555–561, 1992.
18. Heimbach DM, and Waeckerle JF. Inhalation injuries. *Ann Emerg Med* 17: 1316–1320, 1988.
19. Huen AC, Park JK, Godsel LM, Chen X, Bannon LJ, Amargo EV, Hudson TY, Mongiu AK, Leigh IM, Kelsell DP, Gumbiner BM, and Green KJ. Intermediate filament-membrane attachments function synergistically with actin-dependent contacts to regulate intercellular adhesive strength. *J Cell Biol* 159: 1005–1017, 2002.
20. Hyder CL, Pallari HM, Kochin V, and Eriksson JE. Providing cellular signposts: Post-translational modifications of intermediate filaments. *FEBS Lett*. 582: 2140–2148, 2008.
21. Ishii K, Harada R, Matsuo I, Shirakata Y, Hashimoto K, and Amagai M. *In vitro* keratinocyte dissociation assay for evaluation of the pathogenicity of anti-desmoglein 3 IgG autoantibodies in pemphigus vulgaris. *J Invest Dermatol* 124: 939–946, 2005.
22. Ivaska J, Pallari HM, Nevo J, and Eriksson JE. Novel functions of vimentin in cell adhesion, migration, and signaling. *Exp Cell Res*, 2050–2062, 2007.
23. Kiffin R, Christian C, Knecht E, and Cuervo AM. Activation of chaperone-mediated autophagy during oxidative stress. *Mol Biol Cell* 15: 4829–4840, 2004.
24. Kim S and Coulombe PS. Intermediate filament scaffolds fulfill mechanical, organizational, and signaling functions in the cytoplasm. *Genes Dev* 21: 1581–1597, 2007.
25. Kueper T, Grune T, Prahl S, Lenz H, Welge V, Biernoth T, Vogt Y, Muhr GM, Gaemlich A, Jung T, Boemke G, Elsässer HP, Wittern KP, Wenck H, Stäb F, and Blatt T. Vimentin is the specific target in skin glycation. Structural prerequisites, functional consequences, and role in skin aging. *J Biol Chem* 282: 23427–23436, 2007.
26. Lambert C, McCue J, Portas M, Ouyang Y, Li J, Rosano TG, Lazis A, and Freed BM. Acrolein in cigarette smoke inhibits T-cell responses. *J Allergy Clin Immunol* 116: 916–922, 2005.
27. Liao J, Lowthert LA, Ghori N, and Omary MB. The 70-kDa heat shock proteins associate with glandular intermediate filaments in an ATP-dependent manner. *J Biol Chem* 270: 915–922, 1995.
28. Lin D, Saleh S, and Liebler DC. Reversibility of covalent electrophile-protein adducts and chemical toxicity. *Chem Res Toxicol* 21: 2361–2369, 2008.
29. Lopachin RM, Barber DS, Geohagen BC, Gavin T, He D, and Das S. Structure-toxicity analysis of type-2 alkenes: *In vitro* neurotoxicity. *Toxicol Sci* 95: 136–146, 2007.
30. LoPachin RM, Barber DS, and Gavin T. Molecular mechanisms of the conjugated α,β-unsaturated carbonyl derivatives: Relevance to neurotoxicity and neurodegenerative diseases. *Toxicol Sci* 104: 235–249, 2008.
31. Luo J, Hill BG, Gu Y, Cai J, Srivastava S, Bhatnagar A, and Prabhu SD. Mechanisms of acrolein-induced myocardial dysfunction: Implications for environmental and endogenous aldehyde exposure. *Am J Physiol Heart Circ Physiol* 293: H3673–3684, 2007.
32. Magin TM, Vijayaraj P, and Leube RE. Structural and regulatory functions of keratins. *Exp Cell Res* 313: 2021–2032, 2007.
33. Matthay MA, Robriquet L, and Fang X. Alveolar epithelium: Role in lung fluid balance and acute lung injury. *Proc Am Thorac Soc* 2: 206–213, 2005.
34. Meier BW, Gomez JD, Zhou A, and Thompson JA. Immunochemical and proteomic analysis of covalent adducts formed by quinone methide tumor promoters in mouse lung epithelial cell lines. *Chem Res Toxicol* 18: 1575–1585, 2005.
35. Mello CF, Sultana R, Piroddi M, Cai J, Pierce WM, Klein JB, and Butterfield DA. Acrolein induces selective protein carbonylation in synaptosomes. *Neuroscience* 147: 674–679, 2007.
36. Miettinen M and Fetsch JF. Distribution of keratins in normal endothelial cells and a spectrum of vascular tumors: implications in tumor diagnosis. *Hum Pathol* 31: 1062–1067, 2000.
37. Morimoto RI. Proteotoxic stress and inducible chaperone networks in neurodegenerative disease and aging. *Genes Dev* 22: 1427–1438, 2008.
38. Omary BB. Intermediate filaments and their associated diseases. *New Eng J Med* 351: 2087–2100, 2004.
39. Omary MB, Ku NO, Tao GZ, Toivola DM, and Liao J. "Heads and tails" of intermediate filament phosphorylation: Multiple sites and functional insights. *Trends Biochem Sci* 31: 383–394, 2006.
40. Oshima, RG. Intermediate filaments: A historical perspective. *Exp Cell Res* 313: 1981–1994, 2007.
41. Pearl LH, Prodromou C, and Workman P. The Hsp90 molecular chaperone: An open and shut case for treatment. *Biochem J* 410: 439–453, 2008.
42. Pekny M and Lane EB. Intermediate filaments and stress. *Exp Cell Res* 313: 2244–2254, 2007.
43. Perkins DN, Pappin DJ, Creasy DM, and Cottrell JS. Probability-based protein identification by searching sequence databases using mass spectrometry data. *Electrophoresis* 20: 3551–3567, 1999.
44. Prodromou C, Panaretou B, Chohan S, Siligardi G, O'Brien R, Ladbury JE, Roe SM, Piper PW, and Pearl LH. The ATPase cycle of Hsp90 drives a molecular 'clamp' via transient dimerization of the N-terminal domains. *EMBO J* 19: 4383–4392, 2000.
45. Thompson CA and Burcham PC. Protein alkylation, transcriptional responses and cytochrome c release during acrolein toxicity in A549 cells: Influence of nucleophilic culture media constituents. *Toxicol In Vitro* 22: 844–853, 2008.
46. Vaughan CK, Piper PW, Pearl LH, and Prodromou C. A common conformationally coupled ATPase mechanism for yeast and human cytoplasmic HSP90s. *FEBS J* 276: 199–209, 2009.
47. Whitehouse M and Beck FW. Irritancy of cyclophosphamide-derived aldehydes (acrolein, chloracetaldehyde) and their effect on lymphocyte distribution *in vivo*: Protective effect of thiols and bisulphite ions. *Agents Actions* 5: 541–548, 1975.
48. Vila A, Tallman KA, Jacobs AT, Liebler DC, Porter NA, and Marnett LJ. Identification of protein targets of 4-hydroxynonenal using click chemistry for ex vivo biotinylation of azido and alkynyl derivatives. *Chem Res Toxicol* 21: 432–444, 2008.
49. Wagner OI, Rammensee S, Korde N, Wen Q, Leterrier JF, and Janmey PA. Softness, strength and self-repair in intermediate filament networks. *Exp Cell Res* 313: 2228–2235, 2007.

50. Zackroff RV, Goldman AE, Jones JC, Steinert PM, and Goldman RD. Isolation and characterization of keratin-like proteins from cultured cells with fibroblastic morphology. *J Cell Biol* 98: 1231–1237, 1984.

Address correspondence to:
Assoc. Prof. Philip C. Burcham
Pharmacology Unit
School of Medicine and Pharmacology
The University of Western Australia
Nedlands, Western Australia, 6009

E-mail: philip.burcham@uwa.edu.au

Date of first submission to ARS Central, August 12, 2009; date of acceptance, August 16, 2009.

Abbreviations Used

ACR = acrolein
BCA = bicinchoninic acid
DPBS = Dulbecco's phosphate buffered saline
Hsp = heat shock protein
IF = intermediate filaments
IFA = intermediate filament-associated

This article has been cited by:

1. Ferrer H.C. Ong, Peter J. Henry, Philip C. Burcham. 2012. Prior exposure to acrolein accelerates pulmonary inflammation in influenza A-infected mice. *Toxicology Letters* **212**:3, 241-251. [CrossRef]
2. Nadia Moretto, Giorgia Volpi, Fiorella Pastore, Fabrizio Facchinetti. 2012. Acrolein effects in pulmonary cells: relevance to chronic obstructive pulmonary disease. *Annals of the New York Academy of Sciences* **1259**:1, 39-46. [CrossRef]
3. Kiflai Bein, George D. Leikauf. 2011. Acrolein - a pulmonary hazard. *Molecular Nutrition & Food Research* n/a-n/a. [CrossRef]
4. Giancarlo Aldini, Marica Orioli, Marina Carini. 2011. Protein modification by acrolein: Relevance to pathological conditions and inhibition by aldehyde sequestering agents. *Molecular Nutrition & Food Research* n/a-n/a. [CrossRef]
5. Yan Baglo, Mirta M. L. Sousa, Geir Slupphaug, Lars Hagen, Sissel Håvåg, Linda Helander, Kamila A. Zub, Hans E. Krokan, Odrun A. Gederaas. 2011. Photodynamic therapy with hexyl aminolevulinate induces carbonylation, posttranslational modifications and changed expression of proteins in cell survival and cell death pathways. *Photochemical & Photobiological Sciences* **10**:7, 1137. [CrossRef]
6. Yuichiro J. Suzuki , Marina Carini , D. Allan Butterfield . 2010. Protein Carbonylation. *Antioxidants & Redox Signaling* **12**:3, 323-325. [Citation] [Full Text HTML] [Full Text PDF] [Full Text PDF with Links]